J|A|C|S
ARTICLES
Published on Web 04/01/2003

Binding Equilibrium Isotope Effects for Glucose at the Catalytic Domain of Human Brain Hexokinase

Brett E. Lewis and Vern L. Schramm*

Contribution from The Albert Einstein College of Medicine, 1300 Morris Park Avenue, Bronx, New York 10461

Received December 19, 2002; E-mail: vern@aecom.yu.edu

Abstract: We have utilized tritium isotope effects to probe the in vitro binding equilibrium between glucose and human brain hexokinase (E.C.2.7.1.1). Replacing a backbone hydrogen atom in glucose with tritium can significantly increase or decrease the equilibrium association constant. Specifically, the equilibrium tritium isotope effects are 1.027 ± 0.002, 0.927 ± 0.0003, 1.027 ± 0.004, 1.051 ± 0.001, 0.988 ± 0.001, and 1.065 ± 0.003 for [1-*t*]-, [2-*t*]-, [3-*t*]-, [4-*t*]-, [5-*t*]-, and [6,6-t_2]glucose, respectively. We have shown that the existence of prebinding equilibrium isotope effects can contribute to binding isotope effect studies but that this effect is insignificant for glucose binding to hexokinase. The binding isotope effects are interpreted in the context of structural studies of hexokinase−glucose complexes. Ab initio calculations on 2-propanol with or without a hydrogen bonding partner, in steric collision with formaldehyde or methane, and on ethanol, cyclohexanol and 1-hydroxymethyl-tetrahydropyran are presented to clarify the magnitude of isotope effects possible in such interactions and the accompanying changes in free energy. Position-specific binding isotope effects provide direct evidence of the partial deprotonation and activation of O6 by Asp657, of other hydrogen bonding interactions with ionic residues, and of the steric compression of CH2 by the backbone carbonyl of Ser603.

Introduction

Isotope effects have been used for a long time to study chemical and enzymatic kinetics,[1−3] transition states,[4−11] vibrational mode relaxation,[12] and equilibria,[13−15] the nature of hyperconjugation[16,17] and ionization,[18−20] and even the nature of hydrophobicity and the hydrophobic effect.[16,21−23] Conversely, workers have used isotope effects on vapor pressure, surface tension, and molar volume to measure their sensitivity in real systems.[24−28] Isotope effects are well-founded in physical chemistry.[29,30] Their measurement and interpretation have yielded valuable information, even permitting the design of transition-state analogues for metabolically important enzymes.[31−33] There has also been some effort, typically with the dehydrogenases, to utilize equilibrium isotope effects to study substrate−enzyme binding interactions in detail;[34−40] these studies have demonstrated the existence of ground-state destabilization, verified by others with spectroscopic methods.[41−45]

(1) Cortes, S. J.; Mega, T. L.; van Etten, R. L. *J. Org. Chem.* **1991**, *56*, 943.
(2) Bennet, A. J.; Sinnott, M. L. *J. Am. Chem. Soc.* **1986**, *108*, 7287.
(3) Paneth, P. Applications of Heavy Atom Isotope Effects. In *Synthesis and Applications of Isotopically Labeled Compounds 1997*; Heys, J. R., Melillo, D. G., Eds.; John Wiley and Sons Ltd: New York, 1998.
(4) Jones, J. P.; Weiss, P. M.; Cleland, W. W. *Biochemistry* **1991**, *30*, 3634.
(5) Cleland, W. W. Isotope Effects: Determination of Enzyme Transition State Structure. In *Enzyme Kinetics and Mechanism, Part D. Developments in Enzyme Dynamics*; Purich, D. L., Ed.; Academic Press: New York, 1995; Vol. 91.
(6) Rising, K. A.; Schramm, V. L. *J. Am. Chem. Soc.* **1997**, *119*, 27.
(7) Chen, X.-Y.; Berti, P. J.; Schramm, V. L. *J. Am. Chem. Soc.* **2000**, *122*, 6527.
(8) Scheuring, J.; Berti, P. J.; Schramm, V. L. *Biochemistry* **1998**, *37*, 2748.
(9) Schramm, V. L.; Horenstein, B. A.; Bagdassarian, C. K.; Schwartz, S. D.; Berti, P. J.; Rising, K. A.; Scheuring, J.; Kline, P. C.; Parkin, D. W.; Merkler, D. J. *Int. J. Quantum Chem.* **1996**, *23*, 1805.
(10) Horenstein, B. A.; Parkin, D. W.; Estupinan, B.; Schramm, V. L. *Biochemistry* **1991**, *30*, 10788.
(11) Lewis, E. S.; Boozer, C. E. *J. Am. Chem. Soc.* **1954**, *76*, 791.
(12) Gambogi, J. E.; L'Esperance, R. P.; Lehmann, K. K.; Pate, B. H.; Scoles, G. *J. Chem. Phys.* **1993**, *98*, 1116.
(13) Anet, F. A. L.; Basus, V. J.; Hewett, A. P. W.; Saunders, M. *J. Am. Chem. Soc.* **1980**, *102*, 3945.
(14) Lewis, B. E.; Schramm, V. L. *J. Am. Chem. Soc.* **2001**, *123*, 1327.
(15) Craig, B. N.; Janssen, M. U.; Wickersham, B. M.; Rabb, D. M.; Chang, P. S.; O'Leary, D. J. *J. Org. Chem.* **1996**, *61*, 9610.
(16) Lewis, E. S. *Tetrahedron* **1959**, *5*, 143.
(17) Shiner, V. J., Jr. *Tetrahedron* **1959**, *5*, 243.
(18) Lewis, E. S.; Boozer, C. E. *J. Am. Chem. Soc.* **1952**, *74*, 6306.
(19) Northcott, D.; Robertson, R. E. *J. Phys. Chem.* **1969**, *73*, 1559.
(20) Heys, J. R. *J. Chromatogr.* **1987**, *407*, 37.
(21) Love, P.; Taft, R. W., Jr.; Wartik, T. *Tetrahedron* **1959**, *5*, 116.
(22) Baweja, R. *J. Liq. Chromatogr.* **1986**, *9*, 2609.
(23) Tanaka, N.; Thornton, E. R. *J. Am. Chem. Soc.* **1976**, *98*, 1617.
(24) Barnett, J. E. G.; Corina, D. L. *Carbohydr. Res.* **1966**, *3*, 134.
(25) Dixon, J. A.; Schiessler, R. W. *J. Am. Chem. Soc.* **1954**, *76*, 2197.
(26) Bigeleisen, J.; Stern, M. J.; van Hook, W. A. *J. Chem. Phys.* **1963**, *38*, 497.
(27) Bigeleisen, J. *Adv. Chem. Phys.* **1958**, *1*, 1.
(28) Sunko, D. E.; Szele, I.; Hehre, W. J. *J. Am. Chem. Soc.* **1977**, *99*, 5000.
(29) Bigeleisen, J.; Wolfsberg, M. *Adv. Chem. Phys.* **1958**, *1*, 15.
(30) Melander, L. *Isotope Effects on Reaction Rates*; The Ronald Press Company: New York, 1960.
(31) Klimek, F.; Bannasch, P. *Carcinogenesis* **1993**, *14*, 1857.
(32) Kicska, G. A.; Long, L.; Horig, H.; Fairchild, C.; Tyler, P. C.; Furneaux, R. H.; Schramm, V. L.; Kaufman, H. L. *Proc. Natl. Acad. Sci. U.S.A.* **2001**, *98*, 4593.
(33) Schramm, V. L. *Biochim. Biophys. Acta* **2002**, *1587*, 107.
(34) Gawlita, E.; Caldwell, W. S.; O'Leary, M. H.; Paneth, P.; Anderson, V. E. *Biochemistry* **1995**, *34*, 2577.
(35) Gawlita, E.; Paneth, P.; Anderson, V. E. *Biochemistry* **1995**, *34*, 6050.
(36) Gehring, K.; Williams, P. G.; Pelton, J. G.; Morimoto, H.; Wemmer, D. E. *Biochemistry* **1991**, *30*, 5524.
(37) Andersson, L.; MacNeela, J.; Wolfenden, R. *Biochemistry* **1985**, *24*, 330.
(38) Bush, K.; Mahler, H. R.; Shiner, V. J. J. *Science* **1972**, *172*, 478.
(39) LaReau, R. D.; Wan, W.; Anderson, V. E. *Biochemistry* **1989**, *28*, 3619.
(40) Gawlita, E.; Lantz, M.; Paneth, P.; Bell, A.; Tonge, P. J.; Anderson, V. E. *J. Am. Chem. Soc.* **2000**, *122*, 11660.
(41) Kurz, L. C.; Ackerman, J. J. H.; Drysdale, G. R. *Biochemistry* **1985**, *24*, 452.

However, to date there has been no systematic application of isotope effects to the question of hydrogen bonding interactions made between substrate and enzyme in the Michaelis complex. Whereas the nature of deuterium and tritium isotope effects on neighboring group basicity is well-known, its application to binding interactions is largely unknown. Due to the specificity and sensitivity of binding isotope effects, a wealth of information in this area remains to be tapped.

In the present work, we have attempted a systematic analysis of the binding of the most common sugar to its cognate enzyme by measuring binding equilibrium isotope effects and performing computations to model the results.

We explore the binding between glucose and human brain hexokinase [E.C.2.7.1.1] using equilibrium tritium isotope effects. By the omission of $MgATP^{2-}$ from the reaction mixtures, the binary complex is isolated using an ultrafiltration technique, and several large and significant isotope effects have been measured on the association constant. We have used high-level computational chemistry to aid in interpreting these isotope effects, and we have found, with a recent X-ray crystal structure[46] as a starting point, that the binding isotope effects for glucose and human brain hexokinase give direct evidence for substrate nucleophile activation in binding prior to the formation of a ternary complex. Evidence is also presented for direct steric compression of the molecule at CH2 by Ser603 and at CH5 by Asn683.

Materials and Methods

Hexokinase. Subcloning and Expression. *E. coli* BL21(DE3) cells containing pET-11d-mHKI[47] were provided by Dr. Herbert Fromm (Iowa State University) as plated colonies. Contained on this vector was the coding sequence for the (catalytic) C-terminal half of human hexokinase I used in this work. Further manipulations were performed to place an N-terminal 6xHis tag on the expressed hexokinase and to place this construct into a plasmid compatible with cotransfection with the pUBS520-ArgU vector.

Fresh, competent BL21(DE3) cells containing pUBS520-ArgU (plasmid obtained from Prof. Dr. Ralf Mattes, Institut für Industrielle Genetik, Stuttgart, Germany) were transformed with pET-11d-6xHis-mHKI and plated onto LB agar plates supplemented with kanamycin (30 μg/mL) and ampicillin (50 μg/mL). The co-transformation with pUBS520-ArgU resulted in 10-fold higher specific activity of crude cell lysate.

Small-Scale Expression. Cultures were grown at 37 °C in LB supplemented with kanamycin (30 μg/mL) and carbenicillin (50 μg/mL). After addition of overnight inoculum grown in identical conditions, culture densities were permitted to reach an absorbance of 0.8−1.2 at 600 nm and IPTG was added to a 1 mM final concentration. Cultures were incubated at 37 °C for an additional 6−12 h. Cells were harvested by centrifugation and stored briefly at 4 °C. These cells were disrupted by french press into SB buffer (50 mM KPO_4 pH 8.0, 100 mM glucose, 300 mM NaCl, 5 mM β-mercaptoethanol) containing 5 μM phenylmethylsulfonylfluoride (PMSF), and subsequently, the enzyme was purified as described below.

Large-Scale Expression. A large-scale 320 L (80 gallon) fermentor was prepared as described[50] and cleansed with bleach. Sterile-filtered distilled water was added to a volume of 270 L and warmed overnight by circulating tap water through the heating coil. 10X LB media (30 L) was added before 15 L of the overnight inoculum and supplemented with kanamycin (30 mg/L), carbenicillin (25 mg/L), and ampicillin (25 mg/L). Cultures were grown under aerobic conditions at 37 °C to a similar density as previously mentioned and induced with 10 L of 10% lactose. After a 5−10 h incubation, cells were harvested using a Westfalia separator (Centrico, Northvale NJ). In this manner, 1.75 kg of *Escherichia coli* were pelleted. Culture concentrates were frozen to −70 °C as an LB slurry. PMSF was added (final concentration of 5 μM) to thawed cells, and these were disrupted by passing through a Dyno-Mill glass-bead mill (WAB Impandex, Inc, Maywood, NJ).

Enzyme Purification. Purification of hexokinase was performed at 4 °C. Cells broken as previously mentioned were centrifuged at 11 500 rpm for 60 min. Streptomycin sulfate (20% stock solution) was slowly added to the decanted supernatant to a final concentration of 1%, allowed to stir an additional 60 min, and centrifuged at 11 500 for 45 min. Supernatant was decanted and brought to 40% saturation by the addition of solid $(NH_4)_2SO_4$. After the slurry was stirred an additional 60 min, it was centrifuged 9000 rpm for 90 min. Supernatant was brought to 55% saturation by $(NH_4)_2SO_4$ and centrifuged 9000 rpm for 90 min. Pellet was resuspended in minimal volume 50 mM KPO_4 pH 8.0 and dialyzed twice against 100 volumes SB plus 15 mM imidazole (SB-15). Particulates were removed by centrifugation at 6000 rpm for 60 min. Protein was loaded onto an Ni-NTA column (QIAGEN, 30 mL bed volume) which had been pre-equilibrated with SB-15. The column was washed by gravity with 125 mL of SB-15 and then 125 mL of WB-15 buffer (50 mM KPO_4 pH 6.0, 15 mM imidazole, 10% glycerol, 100 mM glucose, 300 mM NaCl, 5 mM β-mercaptoethanol). Hexokinase activity was eluted with a 150 mL gradient of 15−300 mM imidazole in WB. Fractions containing the highest specific activity were pooled and concentrated to ~10 mg/mL. After quick-freezing in a dry ice ethanol bath, aliquots of enzyme were stored at −70 °C.

Enzyme Activity Assay. Activity was measured by a coupled assay via glucose 6-phosphate dehydrogenase by following NAD^+ conversion to NADH at 340 nm as reported elsewhere.[51]

Radiolabeled Glucose. [2-^{14}C]-, [6-^{14}C]-, [1-*t*]-, [2-*t*]-, [3-*t*]-, [5-*t*]-, and [6,6-t_2]glucose materials were obtained from Amersham (Piscataway, NJ) or ARC (St. Louis, MO) and purified as follows. The specific radioactivity of the tritiated glucoses was 10−45 Ci/mmol, and that of the ^{14}C-labeled glucoses was 10−50 mCi/mmol.

[4-*t*]Glucose Synthesis. This procedure was adapted from that of Söderman and Widmalm.[52] NaH (1.5 g, 37.5 mmol) was stirred with methyl 4,6-*O*-benzylidene α-D-glucopyranoside (5 g, 17.5 mmol) (Aldrich, Milwaukee, WI) in 40 mL of dimethylformamide for 6.5 h. Benzyl chloride (4.4 mL) was added and stirred overnight. After the reaction was quenched with methanol and extracted from methylene chloride with 10% HCl, saturated $NaHCO_3$, and brine, pure product methyl 2,3-di-*O*-benzyl-4,6-*O*-benzylidene α-D-glucopyranoside (4.5 g, 9.75 mmol) was recrystallized from methanol. This material (3 g, 6.5 mmol) was added to 1% methanolic HCl. After 1 h at room temperature, TLC (10:1, toluene:ethyl acetate) showed complete conversion to two product bands ($R_f = 0, 0.5$). The reaction was stopped by the addition of saturated $NaHCO_3$ and extracted from methylene chloride with H_2O and brine to yield 2.7 g of crude product. Recrystallization from minimal volume ethyl acetate with hexanes yielded 1.7 g (4.6 mmol) of crystals of pure methyl 2,3-di-*O*-benzyl

(42) Kurz, L. C.; Drysdale, G. R. *Biochemistry* **1987**, *26*, 2623.
(43) Deng, H.; Zheng, J.; Sloan, D.; Burgner, J.; Callender, R. *Biochemistry* **1989**, *28*, 1525.
(44) Deng, H.; Zheng, J.; Sloan, D.; Burgner, J.; Callender, R. *Biochemistry* **1992**, *31*, 5085.
(45) Deng, H.; Burgner, J. W.; Callender, R. H. *J. Am. Chem. Soc.* **1998**, *120*, 4717.
(46) Aleshin, A. E.; Kirby, C.; Liu, X.; Bourenkov, G. P.; Bartunik, H. D.; Fromm, H. J.; Honzatko, R. B. *J. Mol. Biol.* **2000**, *296*, 1001.
(47) Magnani, M.; Bianchi, M.; Casabianca, A.; Stocchi, V.; Daniele, A.; Altruda, F.; Ferrone, M.; Silengo, L. *Biochem. J.* **1992**, *285*, 193.
(48) Aleshin, A. E.; Zeng, C.; Fromm, H. J.; Honzatko, R. B. *FEBS Lett.* **1996**, *391*, 9.
(49) Aleshin, A. E.; Zeng, C.; Bourenkov, G. P.; Bartunik, H. D.; Fromm, H. J.; Honzatko, R. B. *Structure* **1998**, *6*, 39.
(50) Schramm, V. L. *Anal. Biochem.* **1974**, *57*, 377.
(51) Liu, F.; Dong, Q.; Myers, A. M.; Fromm, H. J. *Biochem. Biophys. Res. Comm.* **1991**, *177*, 305.
(52) Soderman, P.; Widmalm, G. *J. Org. Chem.* **1999**, *64*, 4199.

α-D-glucopyranoside. Anhydrous toluene (20 mL) dissolved 1.0 g (2.7 mmol) of this material in the presence of 4 Å molecular sieve beads. After the addition of 682 mg (3.1 mmol) of dibutyl tin oxide, the mixture was refluxed at 130 °C for 3 h and solvent evaporated under reduced pressure. The residue was dissolved in 10 mL of dry chloroform with 385 mg (1.3 mmol) of 1,3-dibromo-5,5-dimethylhydantoin and stirred at room temperature for 20 min. An additional 65 mg (0.22 mmol) of dibromohydantoin was added. After 20 min further, the mixture was extracted from chloroform by 25% (w/v) sodium thiosulfate, H_2O, and brine. Pure methyl 2,3-di-*O*-benzyl-α-D-xylo-hexopyranoside-4-ulose (434 mg, 1.2 mmol) was purified by silica chromatography. The following reduction was performed at the National Tritium Labelling Facility (Berkeley, CA). $NaBH_4$ (0.02 mmol) was added to 1 mL of acetic acid in 5 mL of toluene at 0 °C, combined with 7 Ci (0.100 mmol) $NaBT_4$, and stirring was continued for 20 min at 0 °C before the addition of 39 mg (0.104 mmol) of the ketone. Debenzylation was accomplished via hydrogenation in acetic acid over palladium on activated carbon (10%) for 12 h at 60 psi H_2, followed by filtration and acetic acid and water washing over Celite. Labeled glucose for this study was prepared from the previously mentioned by treatment with α-methylglucosidase and purified with Dionex HPLC as follows.

Radiolabel Purification. Mixtures of ^{14}C-labeled glucose and ^{3}H-labeled glucose were made from stock solutions and evaporated to dryness in a Speed Vac Concentrator (Savant Inc., Hicksville, NY). After reconstitution in 20−40 μL of H_2O, the samples were injected onto high-pH anion exchange HPLC (Dionex Corporation, Sunnyvale, CA) and eluted isocratically at pH 11.7. Fractions in the glucose elution region containing counts were passed over H^+-Dowex 50X8 (200−400), pooled, and concentrated via Speed Vac.

Radiolabel Purity Assay. Approximately 10 000 cpm of each reconstituted sample were added to a final volume of 100 μL of solution containing 12 mM UDP-galactose, 10 mM MgATP, 12.5 mM $MgCl_2$, 50 mM NaCl, 50 mM Tris buffer pH 8.0, and 4 milliunits each of hexokinase, phosphoglucomutase, galactose 1-phosphate uridyltransferase, and UDP-galactose-4-epimerase. After incubating at room temperature for 10 min, the 100 μL sample was loaded onto a "stacked pasteur column" of approximately 1.5 mL of DEAE-sephadex under approximately 1.5 mL of 1:4 charcoal:cellulose. Legitimate counts are converted either into UDP-gal and UDP-glc, retained by charcoal, or into G-6-P and G-1-P, retained by DEAE resin. The columns were washed with 4.1 mL of H_2O, and 1 mL of eluent was added to 10 mL of Liquiscint scintillation fluid (National Diagnostics, Atlanta, GA). This assay/column combination worked quite well; most leaky counts came from DEAE insufficiency and could be minimized. The tolerance permitted for these experiments was defined as

$$\left|\frac{1+(t_{\text{eluted}}/t_{\text{total}})}{1+(^{14}C_{\text{eluted}}/^{14}C_{\text{total}})}-1\right| \le 0.009$$

Binding Isotope Effect (BIE) Experiments. For each experiment, hexokinase dialyzed overnight against 50 mM Tris pH 8.0 with 50 mM NaCl was added to a final concentration of 20−80 μM in three reactions of a 330 μL total volume, pH 8.0, including a 10−50 μM total concentration of ^{3}H- and ^{14}C-labeled sugar, 10 milliunits mutarotase (Calzyme, San Luis Obispo, CA), and 40−80 mM Tris buffer. SpectraPor dialysis membrane leached of metals by boiling in 1 mM EDTA for 15 min was sandwiched between two halves of a plastic ultrafiltration apparatus[53] to form a separation between superior and inferior aspects in each of the 22 "wells". After a 10 min equilibration at room temperature, 105 μL of the binding reaction was added to the superior aspect of each of the three separate compartments, and 22 psi N_2 or Ar (gas) was applied to this side for 60−90 min or until approximately 50 μL had passed through the membrane. Isovolumetric samples (usually 25 μL) were taken from the superior and inferior menisci by a 50 μL Hamilton syringe and then washed into a scintillation vial containing 1 mL of H_2O. Scintillation fluid (10 mL) was added, and these samples were counted in a Wallac 1219 scintillation counter (Perkin-Elmer, Gaithersburg, MD) for several cycles of 10 min per sample to obtain ^{3}H and ^{14}C content. These were considered three independent measurements of the binding equilibrium. The isotope effect is calculated as the quotient of the isotope ratio (^{14}C/^{3}H) of bound glucose and the isotope ratio of free glucose. First, according to the equation

$$R_b = \left(\frac{1}{1-f}\right)R_m - \left(\frac{f}{1-f}\right)R_f$$

the isotope ratio in the bound-glucose pool (R_b) was extrapolated from the isotope ratios in the free-glucose pool (R_f, measured below the membrane) and in the mixed-glucose pool (R_m, measured above the membrane, containing enzyme-bound glucose and free glucose). The fraction of tritiated glucose which remains unbound (f) in the mixed equilibrium above the membrane is taken as the ratio of tritium counts below to tritium counts above the membrane. Controls in triplicate for substrate filtration by the membrane or filtration isotope effect consisted of duplicate wells without hexokinase. Wells lacking enzyme or enzyme and counts were tested each time.

Semiempirical, Ab Initio, and DFT Calculations. A. 2-Propanol. NBO calculations[54] were made in Gaussian[55] from completed geometry-optimization checkpoint files through the inclusion of pop(nbo, full) keywords. Unless otherwise noted, all calculations shown were performed at the density functional level of theory using b3pw91/6-31g**. Some calculations shown were performed at the semiempirical level (pm3) or Hartree−Fock level (rhf/3-21g or rhf/6-31g**). CH-bond stretching mode contribution to overall equilibrium isotope effects (EIE) was made by following the partition function

$$q_{\text{vib}} = h\bar{\nu}/(2k_BT\sinh(h\bar{\nu}/2k_BT))$$

for all frequencies between roughly 2000 and 4000 cm^{-1} while changing the parameter of interest (i.e., HCOH torsional angle) and comparing this value with the overall calculated EIE over the same parameter range.[30]

B. 2-Propanol with Formate and Formic Acid. The parameter scan described for 2-propanol alone (previously mentioned) was performed in the presence of a proton donor (formic acid) or a proton acceptor (formate ion), and the hydrogen bond partner (see Figure 1) was permitted to follow the scanned torsional angle appropriately. Certain parameters were constrained to ensure reasonable analogy between structures as HCOH torsional angle was stepped, including at all times $C_{c,iso}-O_{iso}-O_{form}-C_{form}$: formate (constrained), $C_{c,iso}-O_{iso}-C_{formate}$; formate, $O_{iso}-O_{formate}-C_{formate}-H_{formate}$; formic acid (constrained), $O_{iso}-O_{formic}-C_{formic}-O_{formic}$, $C_{c,iso}-O_{iso}-C_{formic}$; and formic acid, $O_{iso}-O_{formic}-C_{formic}-H_{formic}$. Fixing the COC angle in the "constrained" models prohibited the approach of any part of the formic molecule to within van der Waals distance of H_c, whereas the "loose" models permitted such an approach. The difference made by such a constraint

(53) Schramm, V. L. *J. Biol. Chem.* **1976**, *251*, 3417.

(54) Glendening, E. D.; Reed, A. E.; Carpenter, J. E.; Weinhold, F. *NBO*, version 3.0; University of Wisconsin, 1994.

(55) Frisch, M. J.; Trucks, G. W.; Schlegel, H. B.; Scuseria, G. E.; Robb, M. A.; Cheeseman, J. R.; Zakrzewski, V. G.; Montgomery, J. A.; Stratmann, R. E.; Burant, J. C.; Dapprich, S.; Millam, J. M.; Daniels, A. D.; Kudin, K. N.; Strain, M. C.; Farkas, O.; Tomasi, J.; Barone, V.; Cossi, M.; Cammi, R.; Mennucci, B.; Pomelli, C.; Adamo, C.; Clifford, S.; Ochterski, J.; Petersson, G. A.; Ayala, P. Y.; Cui, Q.; Morokuma, K.; Malick, D. K.; Rabuck, A. D.; Raghavachari, K.; Foresman, J. B.; Cioslowski, J.; Ortiz, J. V.; Stefanov, B. B.; Liu, G.; Liashenko, A.; Piskorz, P.; Komaromi, I.; Gomperts, R.; Martin, R. L.; Fox, D. J.; Keith, T.; Al-Laham, M. A.; Peng, C. Y.; Nanayakkara, A.; Gonzalez, C.; Challacombe, M.; Gill, P. M. W.; Johnson, B. G.; Chen, W.; Wong, M. W.; Andres, J. L.; Head-Gordon, M.; Replogle, E. S.; Pople, J. A. *Gaussian 94*, revisions C.2, D.4, *Gaussian 98*, revision A.6; Gaussian, Inc.: Pittsburgh, PA, 1998.

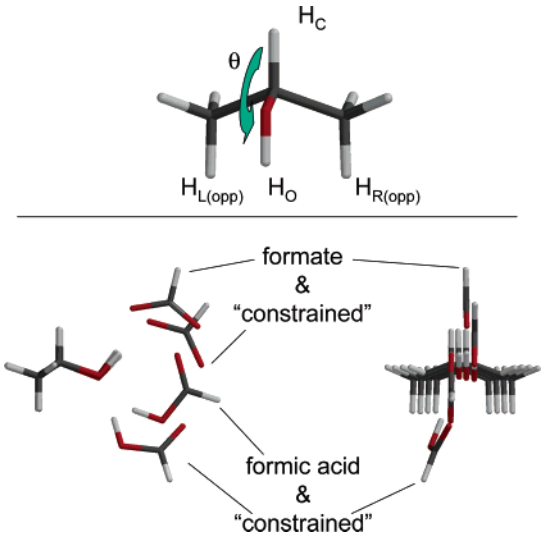

Figure 1. Summary of gas-phase calculations on 2-propanol with hydrogen bonding partners. Upper panel defines torsional angle θ which was subject to the scan from 180° (shown) to 0°. Lower panel shows a side or front view of the difference between constraints used. C−O−C angles were fixed as shown in the "constrained" models but not in regular models. Notably, "regular" formic acid prefers the configuration permitting two hydrogen bonds, while the "constrained" formic acid appears offset by ~15° from coplanarity with the hydroxyl and central carbon as in the other models.

can be seen below. The OOCX and COOC constraints were required to prevent undesirable twisting motions.

Hydrogen bonding distance was explored using 2-propanol at an HCOH angle of either 0° or 180° and formate or formic acid. The HCOH torsional angle was fixed, and the hydrogen bond partner was permitted to find a twist-prohibited energetically minimized hydrogen bonding distance. The O−O distance was then stepped closer or further, each time performing limited energetic minimization. Interaction energy and isotope effect were determined for each distance.

C. 1-Methoxy-tetrahydropyran. To simulate rotation about the C5−C6 bond in glucose, rotations were performed for either (the equivalent of) [5-*t*]- or [6,6-t_2]glucose molecules.

D. 2-Propanol and Formaldehyde Collision. To simulate isotope effects arising from the interaction between the active site residue Ser603 and the CH2 bond in glucose, formaldehyde was positioned near the central CH bond of 2-propanol and then brought closer in a stepwise fashion. The axial collision was modeled by fixing $C_c-H_c-O_{formaldehyde}$ linearly and by fixing $H_c-O_{formaldehyde}-C_{formaldehyde}$ and $H_c-C_{formaldehyde}-H_{formaldehyde}$ at 90° and $O_{iso}-C_c-H_c-C_{formaldehyde}$ at 180°. The starting structure is seen in Figure 7, upper left panel. The approach was modeled by stepping the $H_c-O_{formaldehyde}$ distance down by 0.2 Å beginning at 3.5 Å.

E. Ethanol. A 180° scan in the C1−O1 torsional angle simulates rotation about C6−O6 in glucose. This calculation was performed upon [1,1-t_2]ethanol in the absence of any hydrogen bond partner.

F. Cyclohexanol. Simulating molecular stresses imposed by enzymic binding required the use of cyclohexanol (see Figure 10). The directions explored were "upward" and "downward" in 2° increments to 30° from equilibrium position and "perpendicular to HCO plane" in 2° increments to 20° from equilibrium position for HCOH angles of 0°, 90°, or 180° and tritiations at H_c, H_{left}, and H_{right}. Intramolecular constraints were introduced to limit unwanted contributions from puckering changes and so forth. (Energetic results must be interpreted in light of these constraints, but the same is not necessarily true for isotope effect results.) The HCOH torsional angle was always held fixed, and certain torsional angles including the hydroxyl oxygen were stepped incrementally as previously mentioned. The numerous constraints can be found in the Supporting Information.

Table 1. Experimental Equilibrium Binding Isotope Effects for Glucose and Brain Hexokinase (C-Terminal Mutant)

label	BIE	*n*
[1-*t*] + [2- or 6-^{14}C]glucose	1.027 ± 0.002	9
[2-*t*] + [2- or 6-^{14}C]glucose	0.927 ± 0.0003	60
[3-*t*] + [2- or 6-^{14}C]glucose	1.027 ± 0.004	18
[4-*t*] + [2- or 6-^{14}C]glucose	1.051 ± 0.001	9
[5-*t*] + [2- or 6-^{14}C]glucose	0.988 ± 0.001	9
[6,6-t_2] + [2-^{14}C]glucose	1.065 ± 0.003	18

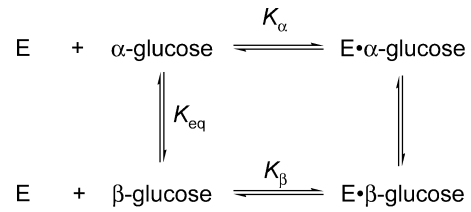

Figure 2. Hexokinase binds either anomer of glucose.

Results

Experimental Glucose−Hexokinase Equilibrium Binding Isotope Effects. In this study, we are probing the vibrational changes occurring in the binding of glucose to human brain hexokinase. The binding isotope effect data are listed in Table 1. These numbers represent the isotopic effect on association; therefore, a value > 1 ("normal isotope effect") indicates that the ^{1}H-glucose binds more tightly than ^{3}H-glucose, and a value < 1 ("inverse effect"), that ^{1}H-glucose binds less well. These effects are indicative of vibrational differences between glucose in solution and glucose bound to hexokinase, where a "tighter" state will favor binding of the glucose with the tritium label. A normal effect, as for [1-*t*], means that the ^{3}H material prefers not to bind as well and that the vibrational environment of the labeled atom is tighter off the enzyme and more loose when bound. The chemical reasons for such vibrational changes are explored in the following computationally with glucose and model compounds.

The largest effects observed were 0.927 for [2-*t*]glucose, 1.051 for [4-*t*]glucose, and 1.065 for [6,6-t_2]glucose, with normal effects of 1.027 for [1-*t*]- and [3-*t*]glucose experiments and the inverse 0.988 for [5-*t*]glucose. These values are quite large and indicate significant vibrational changes experienced by every backbone hydrogen atom in glucose. The error values achievable in this kind of experiment are similar to those observed in kinetic isotope effect studies.

In the binding isotope effect experiments, filtration controls consistently showed a slight (~1%) retention of substrate by the dialysis membrane and also a very slight but significant (0.997−1.000) isotope effect on filtration. The latter we attribute to the different size exclusion behavior expected between the two hydrogen isotopes. This effect adds some error which is already inside our error range, and therefore, the data presented here are corrected only for filtration and not for filtration isotope effect.

Relevance of Anomeric Equilibrium to Glucose BIE. It is possible in this kind of equilibrium study that the existence of an isotope-partitioning equilibrium between several unbound conformers or isomers may contribute significantly to the observed binding isotope effect. This can be illustrated in light of the complete binding equilibrium shown in Figure 2. Were

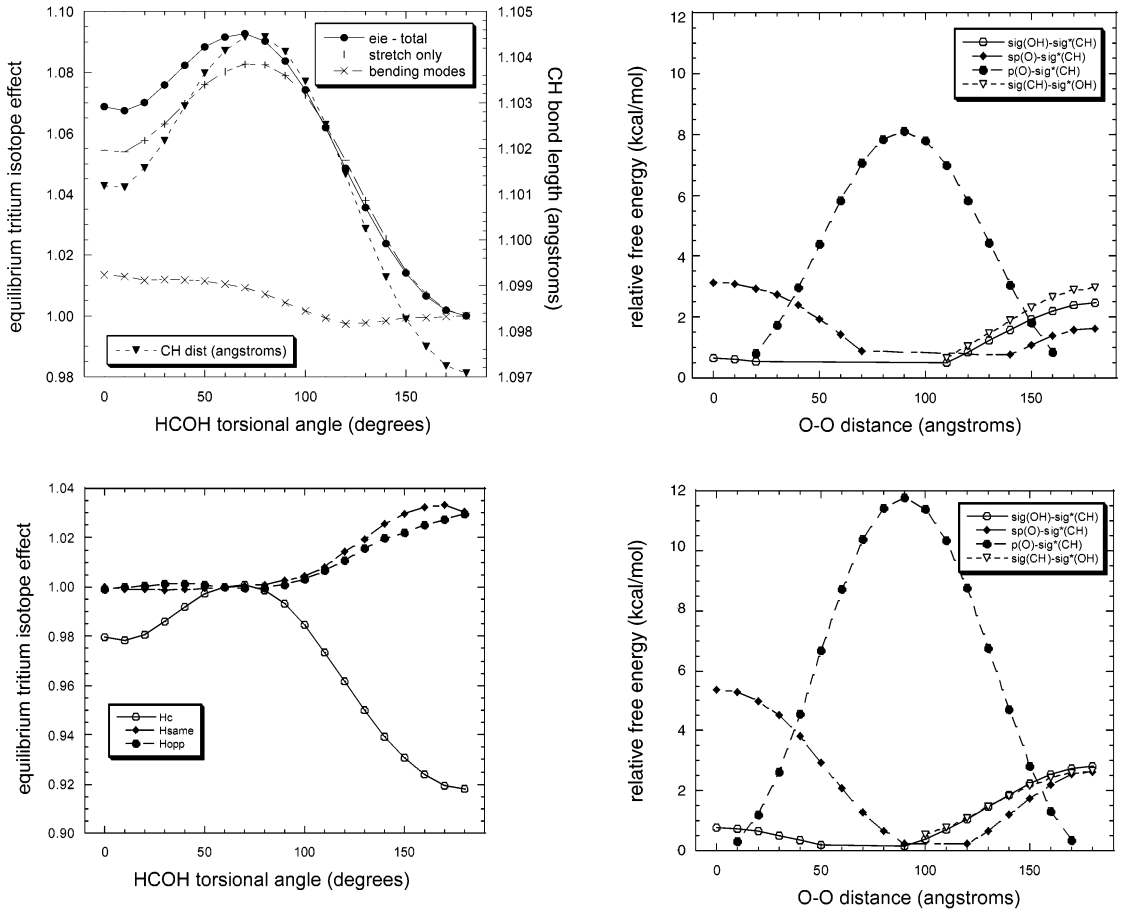

Figure 3. Calculations on 2-propanol and 2-propanol with formate. In 2-propanol, the central CH bond length and isotope effect (upper left) can be compared to hyperconjugations involving this bond (upper right). The latter are magnified by hydrogen bonding with formate ion (lower right). The lower left panel illustrates that, in 2-propanol alone, H_C as well as the antiperiplanar CH bonds are affected by the hydroxyl torsional angle.

a normal equilibrium isotope effect to exist in the anomeric exchange reaction between α- and β-glucose, indicating that the heavy-labeled equilibriums were pushed toward the α-sugar, we would expect the total free α-sugar to be slightly enriched in the heavy label with respect to the total free β-sugar. If hexokinase were to bind α-glucose more tightly, we would observe that the total bound glucose pool would be enriched in heavy label, even in the absence of enzymic isotopic preference.

Therefore, we must account for any anomeric equilibrium isotope effects and measure the relative affinity of α- or β-sugar for the enzyme active site. Presently, we have determined from fluorescence titration with recrystallized α- and β-glucose that $K_\alpha = 15.4 \pm 3.0$ μM and $K_\beta = 23.7 \pm 3.1$ μM.

The anomeric equilibrium isotope effects were obtained previously as deuterium isotope effects[14] and are shown in the first column of Table 2 as the corresponding tritium isotope effects. The ratio of K_α to K_β is 0.65, and the corresponding contribution of this prebinding equilibrium to the observed isotope effects is listed in the column headed by that number. For the purpose of illustration only, the other columns correspond to hypothetical values of the affinity ratio. The table shows that one would require an affinity ratio of 100 to generate an effect close to the experimental binding isotope effect at H1 and a value of less than 0.01 to achieve the binding effect at H2. At the established affinity ratio of 0.65, the isotope effects on anomeric equilibrium do not contribute significantly to binding isotope effects. Therefore the experimental binding isotope effects must result from isotopic fractionation in enzymic binding.

Table 2. Contribution to BIE by Anomeric Equilibrium IE in Aqueous Glucose

		K_α/K_β						
label	$^TK_{eq}$[a]	0.01	0.1	0.65[b]	1.0	10	100	BIE[c]
[1-*t*]	1.063	0.964	0.971	0.994	1.000	1.020	1.024	10.27
[2-*t*]	1.039	0.977	0.982	0.996	1.000	1.013	1.015	0.927
[3-*t*]	1.039	0.977	0.982	0.996	1.000	1.013	1.015	1.027
[4-*t*]	1.001	0.999	1.000	1.000	1.000	1.000	1.000	1.051
[5-*t*]	1.053	0.970	0.975	0.995	1.000	1.017	1.020	0.988
[6,6-t_2]	0.997	1.002	1.001	1.000	1.000	1.000	1.000	1.065

[a] Extrapolated from deuterium isotope effects reported in Lewis and Schramm[14] by the Swain−Schaad relationship. [b] Determined for this system by fluorescence titration. [c] Experimental from Table 1.

Calculations on 2-Propanol. The angle representing hydroxyl orientation (HCOH torsional angle) causes significant changes in both CH bond stretching and bending force constants. Figure 3 (upper left panel) illustrates this angular variation in the overall equilibrium isotope effect (●) as well as its stretching (+) or bending components (×). The stretching isotope effect comprises the main portion of the overall effect and possesses the same general shape as the variation in CH bond length (▼). The peak of these curves occurs between 70° and 80°, roughly corresponding to maximal hyperconjugative electron transfer seen at 90° in the upper right panel of the same figure.

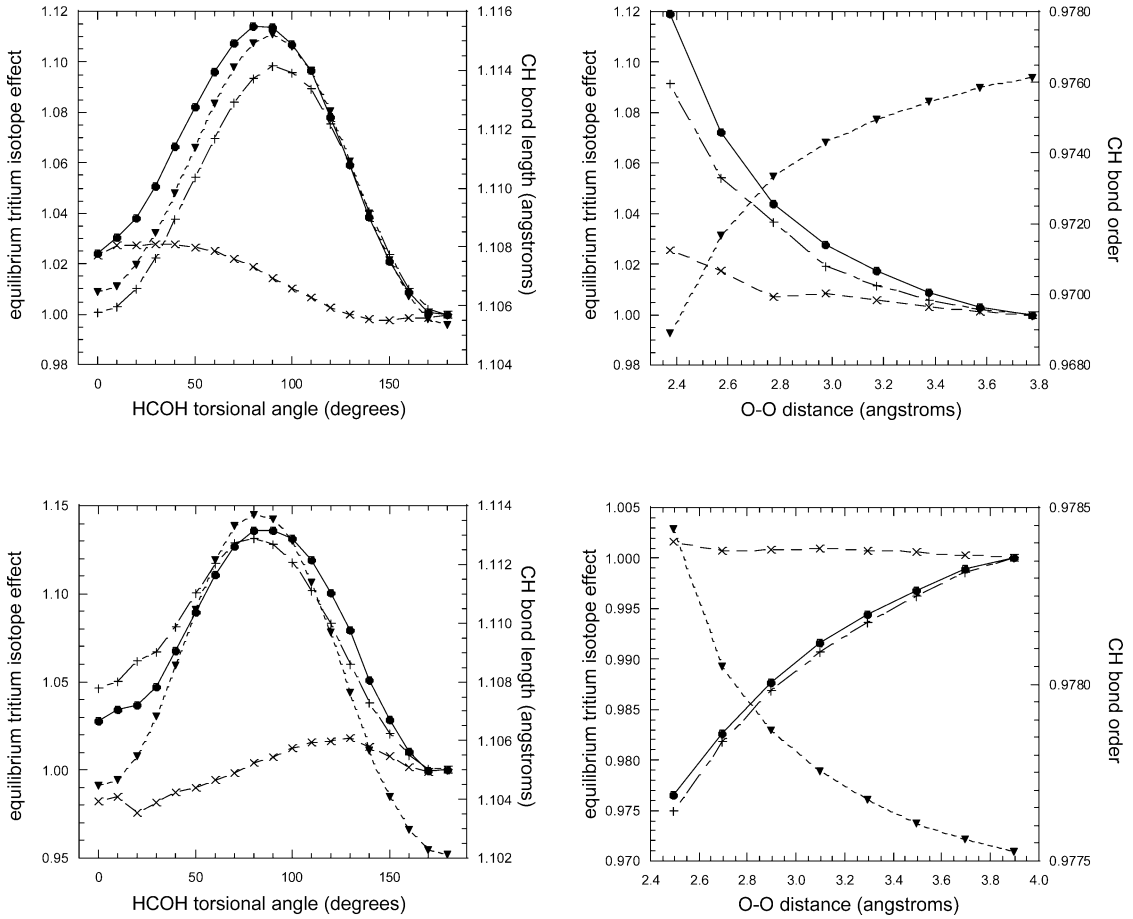

Figure 4. Calculations on 2-propanol demonstrate that both the HCOH torsional angle (left column) and heteroatom distance (right column) cause an isotope effect at H_C when hydrogen-bonded to formate (top row and bottom left) or formic acid (bottom right). Shown is the isotope effect (●) in its components: stretching mode (+) and all other modes (×). CH bond length or CH bond order is also shown (▼).

The nature of this powerful effect is $n_p \rightarrow \sigma^*$ delocalization of the p-type oxygen electron lone pair into the CH bond antibonding orbital (σ^*). By an increase in population in the antibonding orbital, this process lowers CH bond order and lowers (loosens) the stretching force constant. The stretching modes, isotope effect and CH bond length curves are asymmetric, whereas the p-type hyperconjugation is symmetric, indicating that at 0° and 180° hyperconjugation from the sp-type oxygen lone pair (◆) is a much more powerful factor in bond order than $\sigma \rightarrow \sigma^*$ interactions between the planar or antiperiplanar CH and OH bonds (○ and ▽, respectively). If p-type transfer were the only factor or if all hyperconjugative transfers were equally competent, the 0° stretching isotope effect would return to unity or be more normal (more loose) at 180° than at 0°.

Bending modes, on the other hand, may reasonably be expected to respond to CH bond length: the shorter the CH bond, the harder to bend, and vice versa. However, neither the bending mode curve (×) in Figure 3 nor corresponding curves (× and ×) in the left panels of Figure 4 possess the shape of the CH bond length curve. Instead, these bending mode curves are proposed to reflect steric imposition by other entities: either p-type or sp-type oxygen lone pairs in Figure 3 and the upper left panel of Figure 4 or formate ion in the lower left panel of that figure. The contributions of bending modes with 2-propanol alone are more inverse at 180° because of the very bulky back lobe of the sp-type oxygen lone pair. The p-type lone pair is less bulky and offers some relief at at 90°, but the small lobe of this sp-type lone pair is the smallest of all, giving the most normal effect at 0°. This gradient in size becomes more pronounced by including formate ion as in Figure 4 (upper left), as partial deprotonation of the 2-propanol hydroxyl should increase the size of the sp-type orbital where it is relevant at 0° and at 180°. Finally, including formate but permitting intermolecular contact at our CH bond (Figure 4, lower left) returns a very inverse isotope effect at the point of its closest approach to our CH bond.

Returning to Figure 3, the lower left panel shows that the CH bonds antiperiplanar to the central bond (refer to Figure 1) are also affected by this angular rotation, asymmetrically to each other and opposite in effect to the central CH bond. Finally, the lower right panel illustrates the almost 50% increase in hyperconjugation energy due to partial deprotonation by the formate ion.

The upper left and lower left panels of Figure 4 demonstrate the effect constraints may have on these calculations. Formate is included in both panels but is constrained away from the CH central bond only in the upper panel. As described above, the bending modes in the lower panel become inverse around 0°, with a similar trend in overall equilibrium isotope effect. The upper right panel illustrates for the formate approach the dependence on O−O distance at an HCOH angle of 0°, and the lower right panel shows the same for the formic acid approach at the same HCOH angle. Bending modes do not

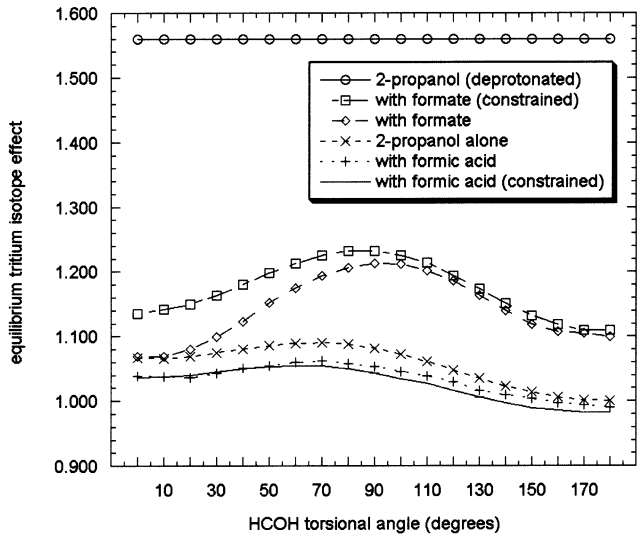

Figure 5. Equilibrium isotope effects on the HCOH torsional angle in 2-propanol with all hydrogen bonding partners studied, normalized for comparison with naked 2-propanol.

change in the latter because the HCOC angle for the formic acid approach always trails the HCOH angle by about 150° (see Figure 1), at HCOH of 0°, the carboxylic acid is too far to affect any kind of steric change. In the former, however, formate's approach at 0° is constrained away from the CH bond as in the upper left panel. This bending mode seems counterintuitive, since we would have expected partial deprotonation to partially rehybridize the small sp-lobe into a slightly more bulky p-type lobe; instead, this loosening may be secondary to the stretching CH bond. The trends in stretching modes and CH bond length should be clear based on previous discussion. Similar calculations have been made for HCOH torsional angles of 180° with similar results (see the Supporting Information for more detail).

All of these individual contributions can be normalized against one another to see the overall angular effect of bringing a hydrogen bond partner into contact with the model hydroxyl. This is shown in Figure 5; all curves are referenced against 2-propanol alone (×), and the effect of full deprotonation (where there is no longer an HCOH angle) is included as well (○). We have seen that partial deprotonation (□ and ◇) always brings a normal isotope effect and partial protonation (+ and ·) always induces a small inverse effect.

All curves can be influenced by steric factors. It should be no surprise that permitting steric contact with the central CH bond would make any hyperconjugative benefit from deprotonation less effective. However, the difference between the formic acid models is not steric (see Figure 1). The less constrained formic acid model permits two hydrogen bonds, the donative one as in the other formic acid model plus a receptive bond. This interaction will partially remove this proton as a formate anion would, yielding a slightly more normal, if still slightly inverse, overall equilibrium isotope effect.

Calculations on Ethanol. Understanding the extracyclic hydroxymethyl OH6 group in glucose requires modeling a 1°-alcohol such as ethanol. The results are illustrated in Figure 6. Glucose molecules used in the experimental portion of this study were doubly tritiated at C6; therefore, we used doubly labeled ethanol. The energetic results (shown in the upper right panel) are as expected with minima at HOCC angles of 60° and 180° for all ab initio methods.

Calculated isotope effects were relatively consistent between models, and we take the DFT results for interpretative purposes. The isotope effect curve shows that the labeled atoms, collectively, possess the lowest force constants at an HOCC angle of 180° and the highest force constants at 90°. As seen previously, this angle-dependent effect derives from the $n \rightarrow \sigma^*$ hyperconjugation which occurs best when the oxygen p-type lone pair crosses the molecule, giving maximal overlap with both CH bonds.

Collision between Formaldehyde and 2-Propanol. Aside from hyperconjugative changes due to conformation and binding, the other major factor in binding isotope effects, particularly inverse isotope effects, is steric imposition. In the binding of glucose to brain hexokinase, we are concerned with the collision of the Ser603 carbonyl with the glucose CH2 bond[49] (see Figure 11).

Therefore, an axial collision between the simplest carbonyl (formaldehyde) and 2-propanol was made in the gas phase. The approach by the formaldehyde oxygen atom was specified along the axis of the central CH bond in 2-propanol, and this axis was set normal to the formaldehyde plane. All models show the expected trend in isotope effect and relative energy except for the semiempirical method, which predicts CH bond lengthening at short approach distances.

By taking the density functional results we found that an approach to within 2.67 Å (as in the crystal structure) produced an inverse isotope effect of approximately 6%, using the intermolecular distance of 3.5 Å as the reference state. The lower right panel of Figure 7 shows the component modes responsible for the overall isotope effect. The overall isotope effect follows bond length; this is a sensible correlation, because decreasing bond length increases bond order and vibrational force constants. However, we would not necessarily expect bond shortening to result from such a collision: Why could not the approach simply affect the CH stretching force constant? Presumably, an approaching oxygen electron cloud would repel and contract the CH bond electrons, thus achieving the bond shortening seen in the figure as well as the approximately equal contributions to the overall isotope effect from stretching and bending modes!

Collision between 2-Propanol and Methane. A study similar to the aforementioned formaldehyde collision was performed by colliding methane axially upon 2-propanol. The results are shown in Figure 8. Surprisingly, with the usual exception of the semiempirical method, the higher the level of theory, the smaller the maximal inverse isotope effect observed. By density functional theory, we expect very little isotope effect from this kind of steric interaction. We conclude that it is difficult to produce a significant isotope effect at H5, despite the presence of an impinging CH group. We may also conclude that reality lies somewhere between Hartree−Fock and density functional theory.

Calculations on 1-Hydroxymethyl-tetrahydropyran (HO-CH_2THP). In glucose, there is a natural degree of freedom arising from rotation about the C5−C6 bond. In solution, this OCCH torsional angle is free to sample many orientations, but it seems from the crystal structure of hexokinase that bound glucose is constrained in this respect. Therefore, we have

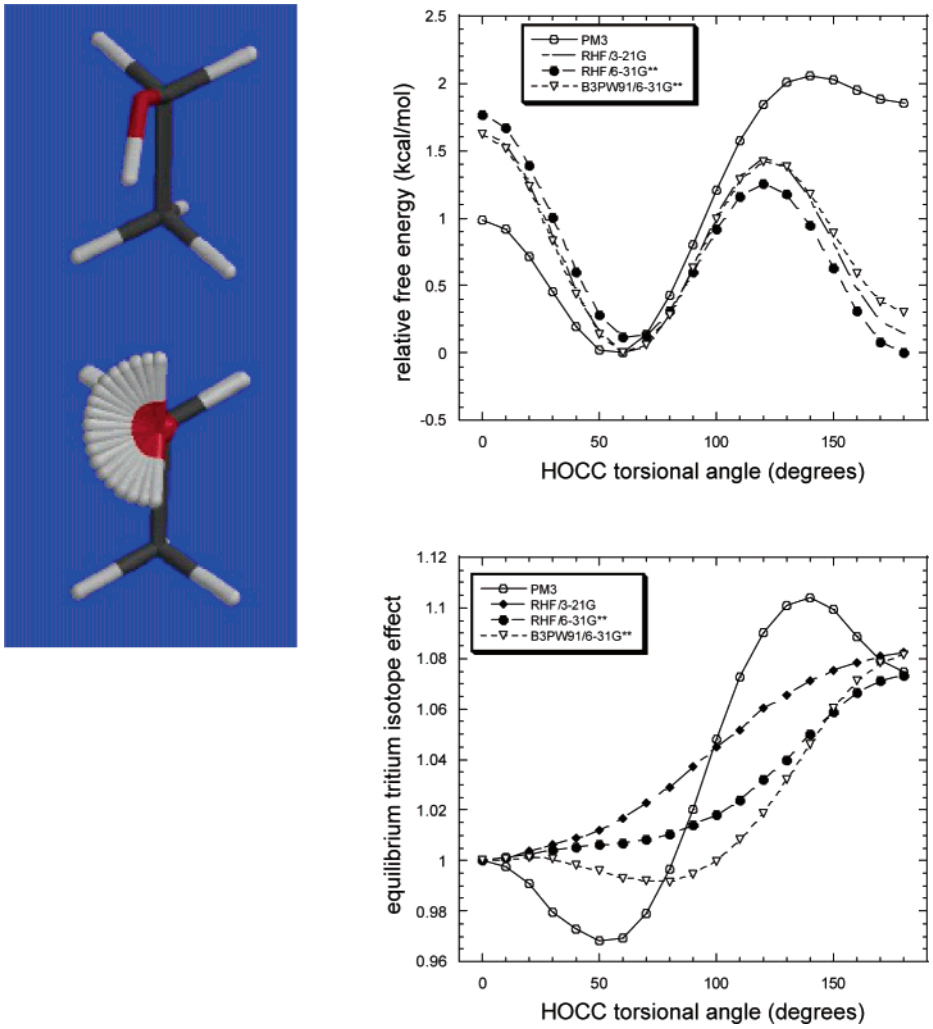

Figure 6. Study of the HOCC torsional angle in ethanol. (Upper right) Relative energy profile for HOCC coordinate. (Lower right) Isotope effect with respect to 0° calculated at pm3, rhf/3-21g, rhf/6-31g**, and b3lyp/6-31g**.

explored this rotation as a possible source of isotope fractionation at H5 and H6.

1-Hydroxymethyl-tetrahydropyran was chosen for its ring oxygen and extracyclic hydroxymethyl group. For simplicity, we number the ring as in glucose, calling the ring oxygen O5 and the primary hydroxyl moiety OH6. The hydroxyl torsional angle HOCC was held fixed at 180° (HOCC contributions were explored in ethanol previously), while the torsional angle O6−C6−C5−H5 was stepped through 360° in 20 increments. The procedure is illustrated in Figure 9 along with energetic and isotope effect results.

Energetically, there exist three minima, at 60°, 180° and 300°, the expected staggered conformations. The area between 180° and 300° is particularly unfavorable in all models due to steric and electrostatic repulsion between the two sets of oxygen lone pairs (probably between both sp-type back lobes).

Isotope effect results for all models indicate that, for both H5 and H6, vibrational laxity occurs at OCCH values of 60°, 180°, and 300°. These are the staggered conformations about C5−C6 and also correspond to antiperiplanar arrangements of H5 with either the H6 atom or O6. The eclipsed conformations vary in tightness as well, but as these are rarely sampled in solution or the present active site, we will not consider them further. At density functional level of theory, there is a maximal difference of about 1.5% isotope effect between highest and lowest staggered peaks for H5 and ∼2% between those for H6. For H5, 180° is the most loose angle, and for H6, 300° is the most loose.

Calculations on Cyclohexanol. It is possible that an enzyme may exert gross strain upon its substrate on binding. Presuming that such an effect would be transmitted through the hydrogen bonds to hydroxyl groups in glucose, we decided to model such effects in a similar cyclic structure containing a hydroxyl group. The cyclohexanol molecule was energetically minimized at HCOH angles of 0°, 90°, and 180° (see Figure 10, upper left panel), and then the hydroxyl group was "pulled" artificially either toward the CH bond ("up"), away from the CH bond ("down"), or perpendicular to the CH bond ("left"). These represent two orthogonal directions which would compose any except for radial strain ("out"), which was not investigated presently. (We would find it unlikely that a molecule surrounded peripherally by hydrogen bond partners could be distorted in any particular direction or that a molecule partially surrounded by hydrogen bond partners would not simply yield in the direction of its pull. Clearly two diametrically opposed bonding partners may impose some effect, however.)

There are three data panels in Figure 10, one for each perturbation direction explored at the density functional level.

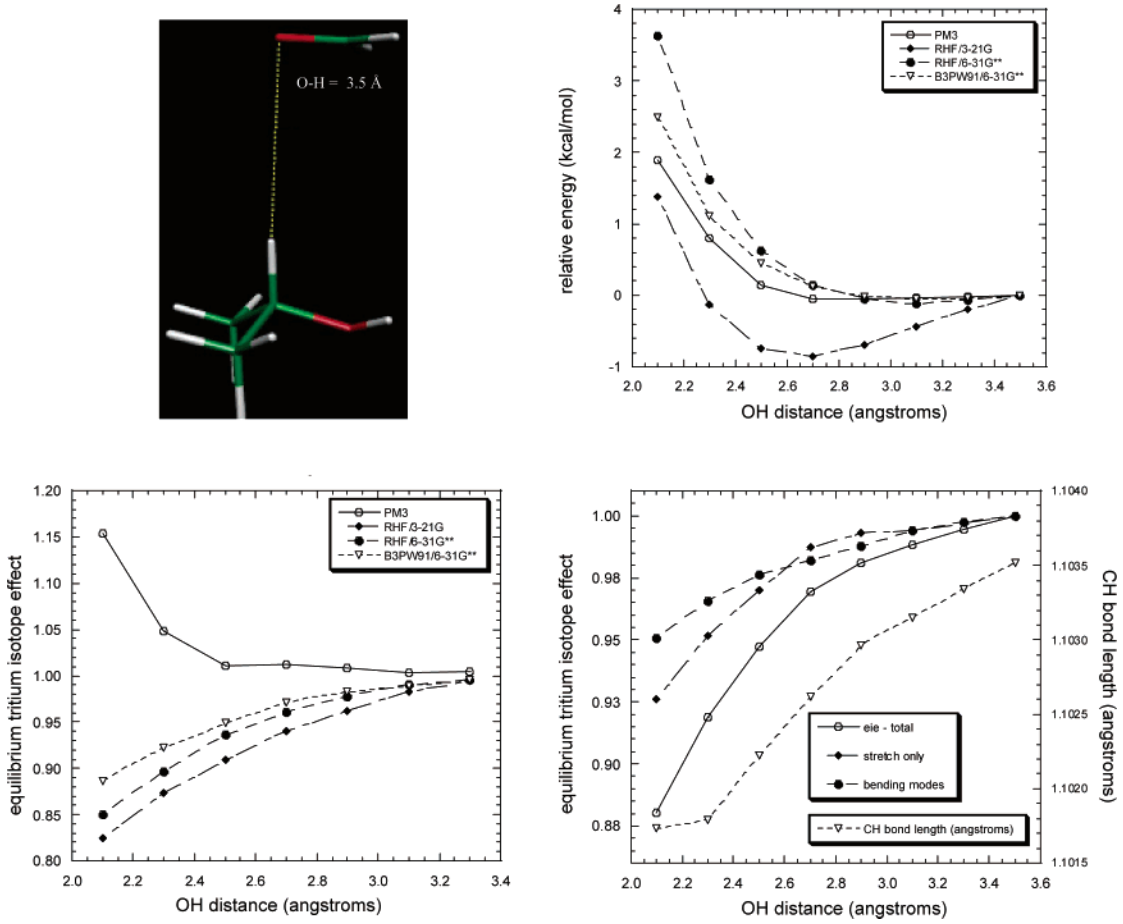

Figure 7. Equilibrium IE for steric imposition of formaldehyde upon 2-propanol. As formaldehyde is brought to impose upon H_C axially (upper left), relative free energy generally increases (upper right panel) and the equilibrium tritium isotope effect becomes strongly inverse (lower left panel). The density functional isotope effect results are expanded to illustrate that stretching and bending modes alike are affected (lower right).

The isotope effect is plotted against the relative energy in kcal/mol of its structure to convey a sense of the strain energy required of the enzyme to produce the observed isotope effect. Taking the lower left panel first, one sees identical curvature for the three fixed HCOH angles. This indicates that, for example, generating a 5% isotope effect from motion which brings the hydroxyl OH bond closer to the geminal CH bond requires about 4 kcal/mol irrespective of the direction the hydroxyl points. However, closer inspection shows that the 180° curve ends at about 5 kcal/mol, well before the other two curves. This indicates that a total upward displacement of 30° from equilibrium in this model costs significantly less than it does for the other two models. Correspondingly, all displacements for the model in this direction cost less than the equivalent displacements in the other two models. All curves indicated inverse isotope effects, probably because of the steric penalty for crowding the CH bond by an OH bond (0°), a p-type lone pair (90°), or the backlobe of an sp-type lone pair (180°). However, the 90° model is probably irrelevant because a hydrogen bonding interaction with this torsional angle is not likely to cause much "up" or "down" vertical displacement.

The lower right panel illustrates isotope effects due to downward motion in the HCO plane. Inverse isotope effects between 2% and 3% can be generated in the 180° model by perturbation all the way to 30° with essentially no energetic requirement (vertical line of closed circles). The 1% normal effect in the 0° model is due to steric relief of OH and CH overlap, followed by the inverse isotope effect seen in the other two models, likely due to uncoupling of the mutually loosening antiperiplanar CH−CH hyperconjugation. Again, the 90° model is not likely to be relevant in any real system.

Whereas "up" and "down" motions mostly reflect rotations about CC bonds on either side of the manipulated OH, the motion resulting in the upper right panel (normal to the HCO plane) represents true distortion of sp^3 hybridization of the central carbon atom. Distortions of this type probably result in a steric relief which would explain the normal isotope effects seen. Here, the 0° and 180° models are probably irrelevant and the 90° model gives insignificant isotope effects even at very high energetic investment.

Discussion

The hexokinases have been subject to study for decades,[56,57] piquing scientific curiosity not only because of the central nature of both substrates, glucose and ATP, but also because the kinetic mechanism has proven particularly elusive.

In pursuing the evaluation of binding isotope effects in this system, it is important to keep in mind that human brain hexokinase (Type I) shares a great deal of similarity and identity not only with the other mammalian hexokinases but also with those of lower organisms. In fact, those residues which contact

(56) Crane, R. K.; Sols, A. *J. Biol. Chem.* **1954**, *210*, 597.
(57) Fromm, H. J.; Zewe, V. *J. Biol. Chem.* **1962**, *237*, 1661.

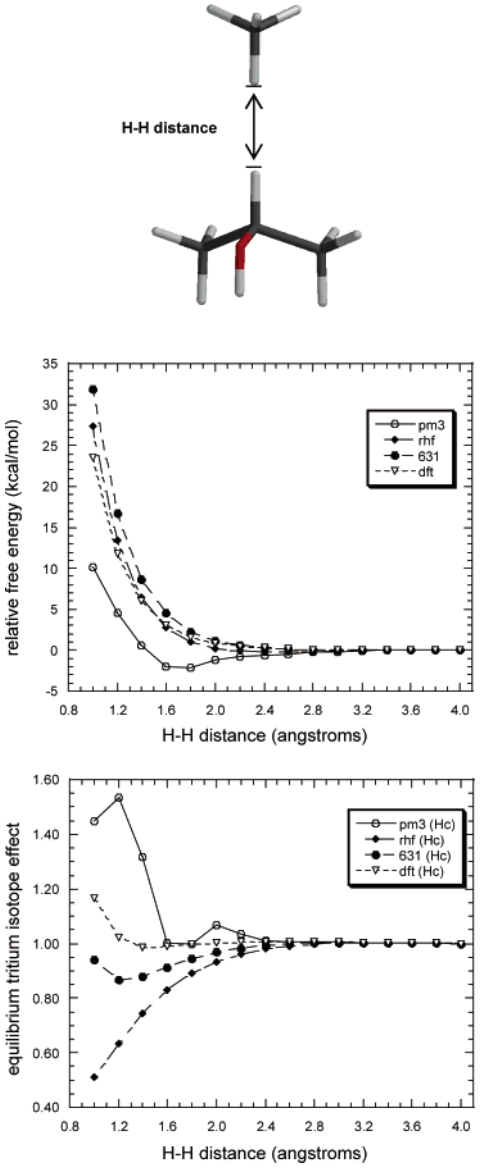

Figure 8. Steric imposition of methane upon 2-propanol. As methane is brought to bear upon H_C axially (top panel), relative free energy generally increases (middle panel) and the isotope effect first becomes inverse then normal. The vibrational loosening seen at very short H−H distances is attributed to the formation of H_2.

glucose in the active site are completely conserved across hexokinase sequences from all isozymes in all species, including those of *Saccharomyces cerevisiae* and *Schistosoma mansoni*. From this we draw two conclusions: first, that evolution has deemed crucial each one of these interactions in terms of both substrate specificity and mechanistic efficiency, and second, that conclusions drawn from this study of human brain hexokinase probably apply to all hexokinases known to date.

Hexokinase−Glucose Active Site. Hexokinase has been shown to possess at least three conformational states leading up to the chemical step. Addition of glucose to yeast hexokinase induces a large conformational change accompanied by a decrease in the radius of gyration[58] and fluorescence,[59−61] by increased thermal stability and interaction between the large and small lobes of the enzyme[62] and by the loss of scores of water molecules.[63] Steitz captured the "open" and "closed" forms of glucose in his famous crystal structures.[64−71] Later, Wilkinson and Rose discovered a third crystal form which released bound glucose more slowly than a crystal corresponding to Steitz' "closed" enzyme,[71] and they proved via isotope trapping that while the "closed" form that Steitz also observed was catalytically incompetent, bound glucose could nonetheless be trapped. Recently, Aleshin et al solved the structure of human brain hexokinase with glucose and ADP bound (1DGK), corresponding to Rose's third form;[46] however, the orientation of the β-PO_4 compelled that group to call for a fourth conformational form, in which the approach of the γ-PO_4 of ATP is not blocked from approaching the 6-hydroxyl of glucose by the enzymic loop present in their ADP structure. Fromm and Honzatko also observed the recombinant brain enzyme in a complex with both glucose and glucose 6-phosphate in the active site (1HKB).[48,49]

We count four different active sites (either 50 kD isozyme or C-terminal subunit) available for inspection: one example of the "open" conformation (2YHK, the addended version of 2YHX[64−69]), actually containing glucose-analogue OTG, one example containing glucose and sulfate (1BDG,[72] and probably the "closed" form 1HKG[71]), four with glucose and glucose 6-phosphate (1HKB,[48,49] 1QHA,[73] 1BG3,[72] and 1CZA[46]), and one example with sugar and ADP bound (1DGK[46]). There are currently no examples of truly glucose-free active sites, glucose-only active sites, and sugar-with-ATP sites. Fortunately, we do not require the first or last of these for the present study, and a closer look at the available structures will lead us to a suitable active site: the only clear difference in the glucose binding site of all available structures lacking nucleotide is that, in the "open" form, the equivalent of Lys621 is missing from the glucose binding pocket. Contact residues appear unmoved by the substitution of phosphate or glucose 6-phosphate.

Therefore, while none represent the glucose-only form, we take them collectively to approximate this structure, and we shall illustrate further points via a 1.9 Å glucose 6-phosphate form (1CZA) in order to make later nucleotide binding easier to imagine. The glucose binding pocket is illustrated in Figure 11. A schematic is shown of all hydrogen bonding contacts, and the active site is shown piecewise.

Existence of Binding Isotope Effects for Glucose and Hexokinase. Contributions from the prebinding equilibrium have been ruled out (see Table 2 and accompanying Results section); therefore, we may interpret the present results in terms of the binding equilibrium itself.

(58) McDonald, R. C.; Steitz, T. A.; Engelman, D. M. *Biochemistry* **1979**, *18*, 338.
(59) Wasylewski, A.; Criscimagna, N. L.; Horowitz, P. M. *Biochim. Biophys. Acta* **1985**, *831*, 201.
(60) Hoggett, J. G.; Kellett, G. L. *Eur. J. Biochem.* **1976**, *66*, 65.
(61) Woolfitt, A. R.; Kellet, G. L.; Hoggett, J. G. *Biochim. Biophys. Acta* **1988**, *952*, 238.
(62) Takahashi, K.; Casey, J. L.; Sturtevant, J. M. *Biochemistry* **1981**, *20*, 4693.
(63) Rand, R. P.; Fuller, N. L.; Butko, P.; Francis, G.; Nicholls, P. *Biochemistry* **1993**, *32*, 5925.
(64) Anderson, W. F.; Fletterick, R. J.; Steitz, T. A. *J. Mol. Biol.* **1974**, *86*, 261.
(65) Anderson, C. M.; Stenkamp, R. E.; McDonald, R. C.; Steitz, T. A. *J. Mol. Biol.* **1978**, *123*, 207.
(66) Anderson, C. M.; Zucker, F. H.; Steitz, T. A. *Science* **1979**, *204*, 375.
(67) Fletterick, R. J.; Bates, D. J.; Steitz, T. A. *Proc. Natl. Acad. Sci. U.S.A.* **1975**, *72*, 38.
(68) Steitz, T. A.; Fletterick, R. J.; Hwang, K. J. *J. Mol. Biol.* **1973**, *78*, 551.
(69) Steitz, T. A.; Anderson, W. F.; Fletterick, R. J.; Anderson, C. M. *J. Biol. Chem.* **1977**, *252*, 4494.
(70) Bennett, W. S. J.; Steitz, T. A. *Proc. Natl. Acad. Sci. U.S.A.* **1978**, *75*, 4848.
(71) Bennett, W. S. J.; Steitz, T. A. *J. Mol. Biol.* **1980**, *140*, 183. Wilkinson, K. D.; Rose, I. A. *J. Biol. Chem.* **1981**, *256*, 9890.

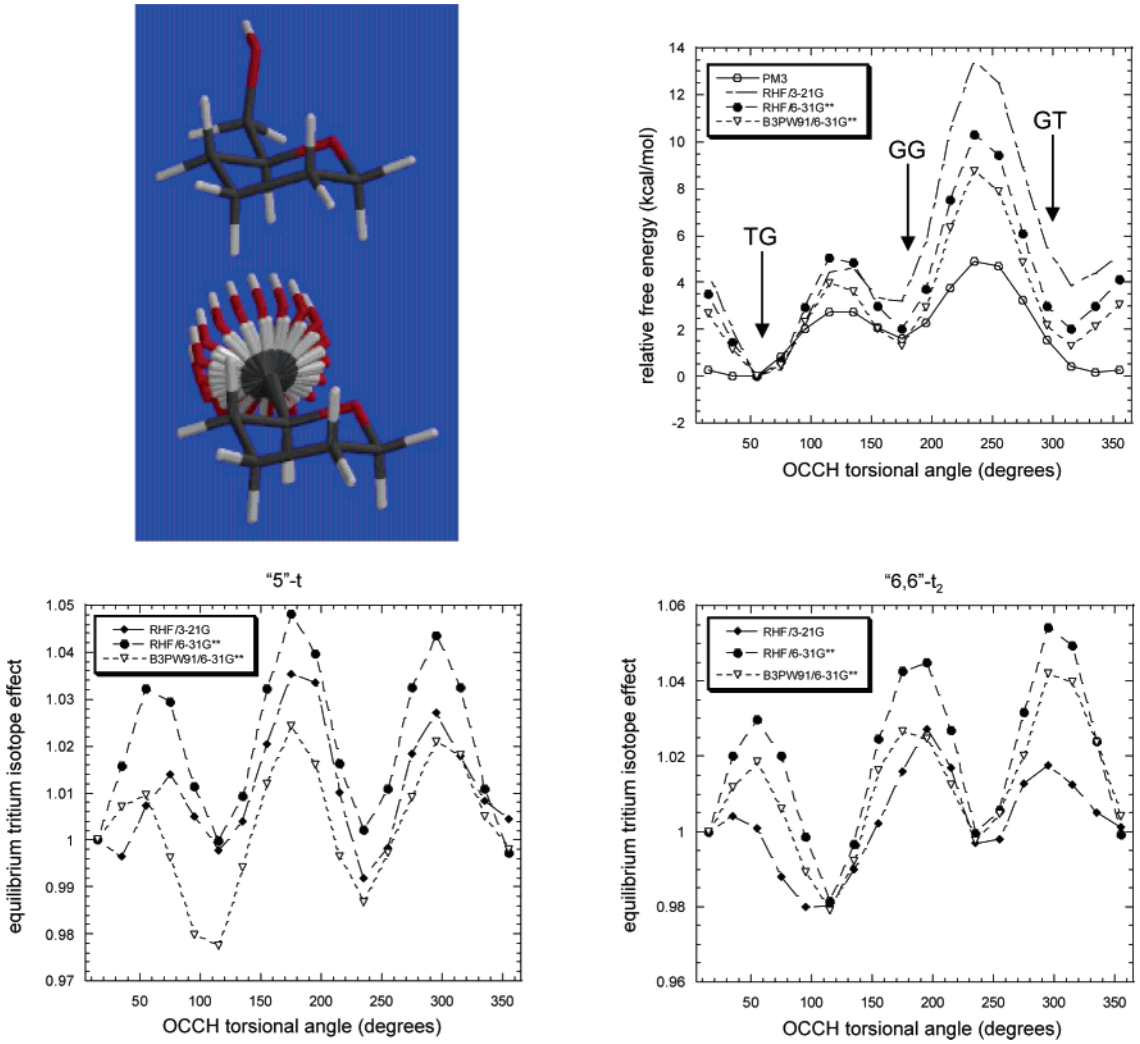

Figure 9. C5−C6 rotation in 1-hydroxymethyl-THP. Rotation about this bond shows energetic minima at staggered conformations (upper right). Isotope effects due to tritiation at "H5" or ditritiation at "H6" indicate that these atoms are the least vibrationally constricted at the staggered conformations as well (lower left and right).

Hydroxyl Torsional Angle Changes. Taking previous conclusions about the preferred hydroxyl torsional angles of glucose in aqueous solution,[14] we may make the comparison to the expected torsional angles due to hydrogen bonding in the active site. The following hydroxyl angles do not change significantly upon binding: OH1 and OH3 each remain at ∼60°; OH2 and OH4 merely flip sign, changing 60° to −60° and −160° to 160°, respectively. There is only one changed angle: that at OH6 (HOCC) changes from approximately −60° to about −120°, giving a normal contribution to the isotope effect at H6 of about 2.5%.

Isotope Effects at H1, H3, and H4. Of all equilibrium isotope effects in this system, the easiest to explain are normal effects; a normal isotope effect at H1 requires only identifying an active site carboxylate within hydrogen bonding distance to OH1. Glu742, Glu708, and Asp657 satisfy this requirement for the normal isotope effects at H1, H3, and H4, respectively. The heteroatom distance study reported in Figure 4 predicts a normal isotope effect of ∼7% at H4 due to the close approach of Asp657. It is unusual, however, that the isotope effects at H1 and H3 should be only 2.7%, since those respective hydroxyls are subject to much tighter hydrogen bonds (although the heteroatom distances reported in ref 46 of 2.38 and 2.45 Å, respectively, are probably too short).

Isotope Effect at H2. Glu708 is within hydrogen bonding distance to OH2 as well as OH3, previously mentioned. Would we then not expect a large normal isotope effect at H2? The key to this surprising result is that the isotope effect at H2 is the resultant of two superimposed effects: hydrogen bonding between the geminal hydroxyl and Glu708 as well as a steric interaction with the backbone carbonyl group of Ser603. Isotope effects are typically multiplicative in nature, so the very inverse total effect at H2 demands a large inverse effect from steric interaction with Ser603. In addition, Glu708 does not approach OH2 as closely as it does OH3, and the latter isotope effect is 1.027, so we expect a small normal contribution to H2 from the presence of Glu708. Density functional calculations on the collision of formaldehyde with 2-propanol predict an inverse ≈ 6% effect for approach to 2.43 Å; the Hartree−Fock calculations demonstrate greater effects at this distance. Therefore, we attribute the very inverse isotope effect at H2 to steric imposition by the backbone carbonyl oxygen of Ser603.

Extracyclic Hydroxymethyl (C5−C6 Bond Rotation). The structure of glucose bound into the active site of hexokinase

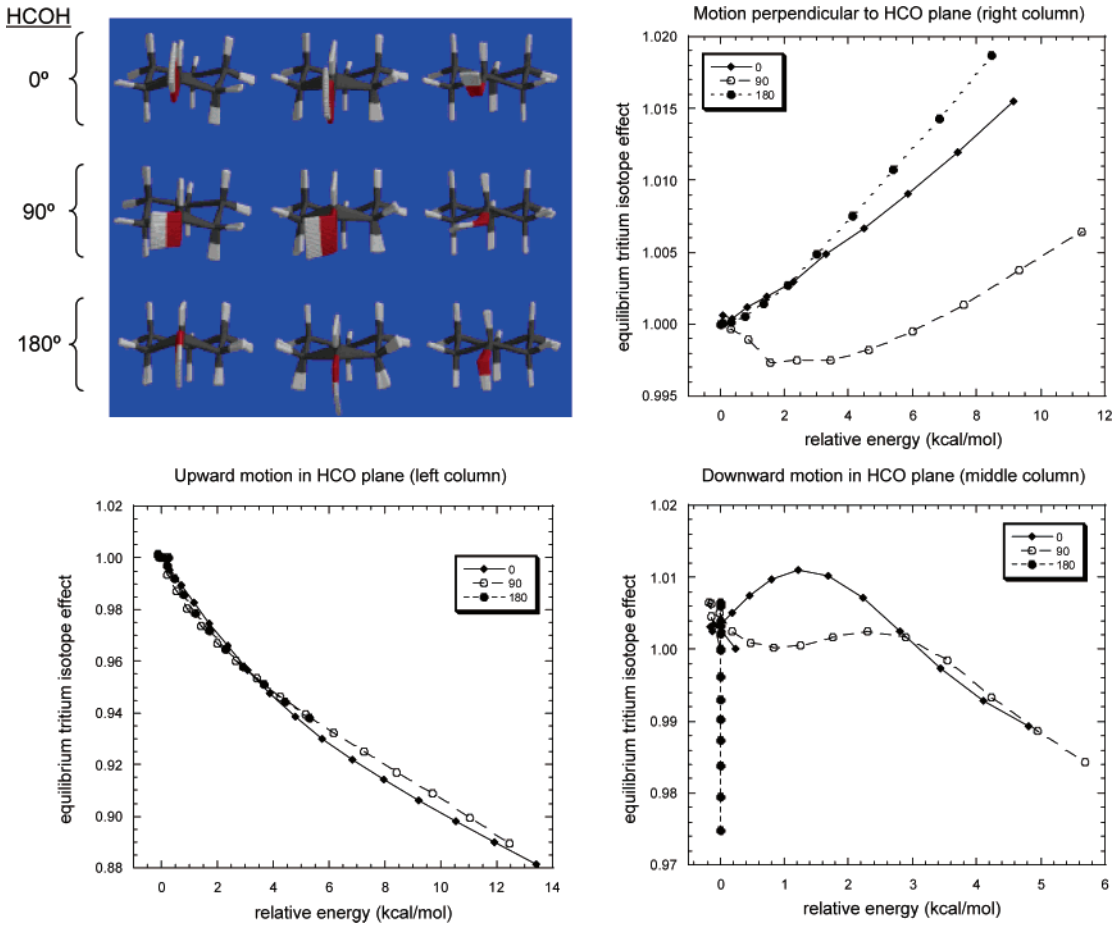

Figure 10. Equilibrium isotope effect studies of cyclohexanol. The upper left panel depicts the three HCOH angles as rows and the perturbations to which these are subjected as columns. The other panels show the energetic investment required to produce a given isotope effect for perturbation in one direction, compared with the HCOH angle.

suggests that the O6−C6−C5−H5 torsional angle is 180° (Figure 11, lower left panel). It is likely that the sugar is permitted very little freedom in this coordinate after binding. For glucose in solution, previous experimental[74] and theoretical[14] work have found that glucose probably prefers this angle to 300° by a ratio of about 55:45, with little contribution from 60°. For the purposes of illustration, these angles are labeled in Figure 9 as GG, GT, and TG, respectively. It should not be of concern that the gas-phase calculated relative energies are reversed in favorability.

These measurements suggest that, in binding to the enzyme active site, a significant proportion of glucose material will have to convert from the GT to the GG conformation. On the basis of the isotope effects calculated in our Figure 9, this mass effect gives a slightly normal contribution to the H5 isotope effect (in going from a lower peak to a higher one, lower left panel) and a slightly inverse one to the H6 effect (lower right panel).

Isotope Effect at H6. Binding to the active site exposes this hydroxyl to the charged residues Asp657 and Lys621; the 6-hydroxyl proton most likely will point directly to Asp657, leaving the electron lone pairs of O6 to engage a donated proton from Lys621 as well as any water molecules present (see Figure

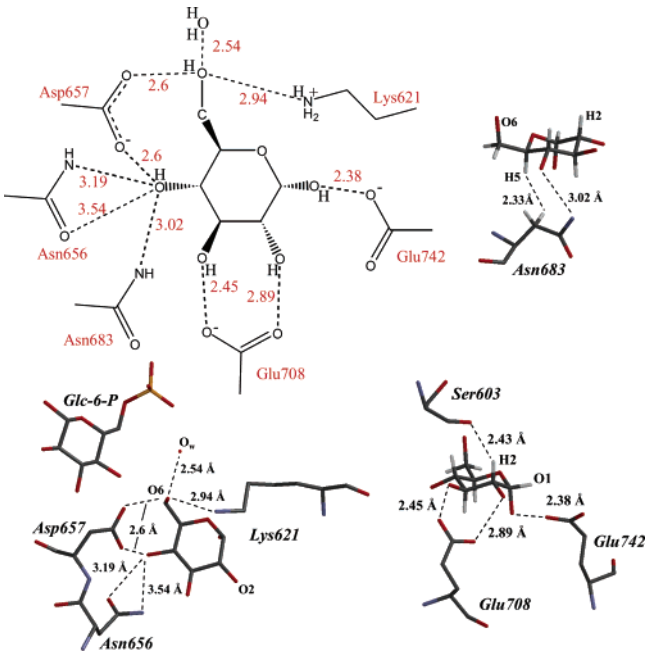

Figure 11. Hydrogen bonding contacts made with glucose (upper left). Shown are a steric contact at H5 (upper right), bonding and steric contacts around H1, H2, and H3 (lower right), and hydrogen bonding contacts at OH6 (lower left). These coordinates are from the 1CZA entry.[46] While the oxygen−oxygen distances of 2.38 and 2.45 Å most likely represent an error in the fitting of electron density, we include the present structural information as published by those authors.

(72) Mulichak, A. M.; Wilson, J. E.; Padmanabhan, K.; Garavito, R. M. *Nat. Struct. Biol.* **1998**, *5*, 555.
(73) Rosano, C.; Sabini, E.; Rizzi, M.; Deriu, D.; Murshudov, G.; Bianchi, M.; Serafini, G.; Magnani, M.; Bolognesi, M. *Structure* **1999**, *7*, 1427.
(74) Nishida, Y.; Ohrui, H.; Meguro, H. *Tetrahedron Lett.* **1984**, *25*, 1575.

11). In solution, OH6 can reasonably be expected to sample HOCC angles randomly but probably unevenly, as gas-phase minima for the primary alcohol occur at 60°, −60°, and 180°. Gas-phase calculations on glucose typically point the HOCC angle toward OH4 (−60°), whereas the present hydrogen bonds give an angle of ∼120°, restricting the isotope effect due to hydroxyl reorientation to a maximum of about 2.5% (see Figure 6). Further, this normal effect will be offset by a slight inverse effect due to attack by the proton donor Lys621. The gap between the large experimental value of 1.065 and the minor contributions from these other effects leaves as the only possibility partial hydroxyl deprotonation by a strong hydrogen bond in the active site. A study conducted in our laboratory has demonstrated the difficulty in ionizing glucose at OH6 as well as the sensitivity of the double label to such a deprotonation (Lewis and Schramm, manuscript in preparation). These observations indicate an increased microscopic pK_a for OH6 with respect to the other hydroxyl groups, implying that a closer and stronger hydrogen bond is necessary to accomplish partial deprotonation. Likewise, poor acidity correlates with strong nucleophilicity. The sensitivity of isotope effects at H6 to deprotonation probably means that future efforts can be made to estimate the binding energy at OH6 and its contribution to ground-state destabilization of glucose.

Finally, the existence of strong OH6 nucleophilicity is supported by the presence of a tight hydrogen bond (2.54 Å) to a water oxygen in the crystal structure at 1.9 Å resolution. The position of this water also implies some directionality to this nucleophilicity, particularly since it lies between O6 and the putative binding pocket for the γ-phosphate of ATP (for a description of the proposed nucleotide binding, see ref 46).

Isotope Effect at H5. We must begin with a slight normal isotope effect on the basis of C5−C6 rotation and another small normal effect at H5 due to the partial deprotonation at OH6 and then determine the source of a larger inverse isotope effect. Density functional theory calculations on the axial approach of methane to the 2-propanol CH bond predicts no isotope effect, and the Hartree−Fock calculations predict at most an inverse 3% isotope effect at an HH distance of 2.33 Å. We notice that the approach of Asn683 to H5 in the crystal structure is not axial, and it is possible for a sideward attack to be more effective in generating an inverse effect. Further calculations at the density functional level are required to fully resolve this discrepancy.

While tightening of modes is responsible for inverse isotope effects, and the H5−C5−C6−O6 libration will probably be tighter on the enzyme, previous calculations have shown insignificant coupling of the hydrogen atom (H5 in this case) with this libration. Instead, the vibrations involving H5 are bending modes and a stretching mode of 800−1800 wavenumbers and 2800 wavenumbers, respectively; hydroxyl torsional librations are typically closer to 280 wavenumbers.

Gross Molecular Strain. Based on the calculations of cyclohexanol (Figure 10), we find it unlikely that gross molecular strain contributes significantly to the observed isotope effects. This is not to say that gross molecular strain does not exist or that it plays no role in this reaction but that the strains large enough to produce an observable isotope effect are energetically unfavorable and such effects are presently dwarfed by the more visible hydrogen bonding effects.

Table 3. Summary of Binding Effects

	hyperconjugative				
position	deprot	hydroxyl angle restriction	C5–C6 rotation	steric compression	total
1	1.027				1.027
2	1.010			0.917	0.927
3	1.027				1.027
4	1.051				1.051
5			1.004	0.984	0.988
6	1.050	1.025	0.990		1.065

Solvation. It is not necessarily the case that binding at an enzyme active site should yield only inverse steric isotope effects. If the structure of water impedes an atom's vibrational motion more than the active site into which it partitions, a normal isotope effect would be seen. However, present information available for the solvation shells of backbone hydrogen atoms in aqueous glucose is not of sufficient resolution to make such a comparison with the active site (see Acknowledgment).

Ground-State Destabilization in the Sugar−Enzyme Binary Complex. It has been shown that, in the ternary complex required for catalysis, the terminal phosphoryl group of ATP is subject to attack by OH6 of glucose with no phosphoenzyme intermediate.[75−77] Evidence for a dissociative transition state has been obtained,[4] and the general base responsible for proton abstraction from OH6 has been identified as Asp657 (in the human sequence).[78] However, the timing of activation of OH6 by Asp657 has not been established.

We propose that the nucleophilic activation of OH6 observed in the present study requires the cooperation of all of the active site residues in order to position that hydroxyl. Indeed, mutations of these other residues affect k_{cat}.[79,80] It is possible that the observed buildup of negative charge on O4 due to tight hydrogen bonding may contribute to the reaction by directionally destabilizing the p-type electron lone pair of O6. It is difficult to tell the orientation of Asn656 or Asn683, but these may play some role in either alleviating a charge buildup or encouraging it. Finally, Lys621 is not often mentioned in discussions of catalysis, but it is positioned where it may help to prevent rotation about the C5−C6 bond in the binary complex.

Kinetic Isotope Effect Studies. Isotope effects on the binding equilibrium can derive from either k_{on} or k_{off}, and we have made no effort in this study to distinguish the two. However, this information can be very important in terms of a kinetic isotope effect study, since, in the limit of the perfect enzyme, we would expect the transition state for the binding reaction not to be much lower in energy than any other transition state, even than the chemical step. In $^{T}(V/K_m)$ studies, the highest energy transition states all contribute to the observed effect, so for very efficient enzymes, it may be necessary to quantitate kinetic binding isotope effects.

Conclusion

Binding isotope effects can be used to determine unequivocally both the protonation state of substrates and active-site

(75) Rose, I. A. *Biochem. Biophys. Res. Commun.* **1980**, *94*, 573.
(76) Orr, G. A.; Simon, J.; Jones, S. R.; Chin, G. J.; Knowles, J. R. *Proc. Natl. Acad. Sci. U.S.A.* **1978**, *75*, 2230.
(77) Blattler, W. A.; Knowles, J. R. *J. Am. Chem. Soc.* **1979**, *101*, 510.
(78) Viola, R. E.; Cleland, W. W. *Biochemistry* **1978**, *17*, 4111.
(79) Arora, K. K.; Filburn, C. R.; Pedersen, C. *J. Biol. Chem.* **1991**, *266*, 5359.
(80) Baijal, M.; Wilson, J. E. *Arch. Biochem. Biophys.* **1992**, *298*, 271.
(81) Molteni, C.; Parrinello, M. *J. Am. Chem. Soc.* **1998**, *120*, 2168.

residues and also the nature of the hydrogen bond network. Experimental binding isotope effect observations can be clouded by isotope effects on prebinding conformational or isomeric equilibria, but we have ruled out this effect in glucose binding to hexokinase. We conclude that the present experimental results indicate ground-state destabilization of glucose upon binding brain hexokinase, detail hydrogen bonding interactions with ionic residues, and reveal steric compression by nonionic groups. The binding isotope effects and their likely phenomenological causes are summarized in Table 3.

It is generally agreed that enzymes accomplish their remarkable rate acceleration by lowering the free energy of the chemical transition state. Many enzymologists have wondered whether binding the enzyme produces a substrate form which is slightly increased in free energy, utilizing binding energy of the whole molecule to impose ground-state activation of the functional part. These data represent evidence of this ground-state destabilization. In a related paper, we show partial relief of ground-state destabilization in the ternary complex with an ATP analogue.[82]

(82) Lewis, B. E.; Schramm, V. L. *J. Am. Chem. Soc.* **2003**, *125*, 4672.

Finally, the authors hope that the present study will call to light both the availability of the experimental methods (already developed[39,53] and refined herein) as well as the arrival of computational power suited for such high-level conformational and distance analyses required to model binding isotope effects in detail.

Acknowledgment. This work was performed in Bronx, NY, and was supported by Research Grant GM41916 from the National Institutes of Health. The authors would like to express deep gratitude to Dr. Kelly Tanaka and to Drs. Phillip Williams and Hiromi Morimoto of the National Tritium Labelling Facility (formerly Berkeley, CA) for their assistance in the synthesis of [4-*t*]glucose. The completion of this work would not have been possible without their help. We also thank Carla Molteni for summarizing and forwarding to us her MM calculations on aqueous glucose,[81] which were not included in this paper.

Supporting Information Available: Cartesian coordinates and constraints used for all models reported here calculated at the density functional level of theory. This material is available free of charge via the Internet at http://pubs.acs.org.

JA0298242